Deuteron nuclear magnetic resonance study of high-pressure effects on the molecular dynamics in amorphous polyethylene

A. S. Kulik† and K. O. Prins*
Van der Waals–Zeeman Laboratory, University of Amsterdam, Valckenierstraat 65/67, NL–1018 XE Amsterdam, The Netherlands
(Received 7 August 1993; revised 4 November 1993)

The effect of high pressure up to 2500 bar on the chain motion in amorphous chain-deuterated polyethylene is studied in a wide range of temperature (203–393 K) using the deuteron nuclear magnetic resonance (^{2}H n.m.r.) quadrupole echo and spin alignment echo technique. Quadrupole echo spectra simulated on the basis of Flory's rotational isomeric state model appear to reproduce the experimental spectra quite well. The comparison yields information on the time-scale of the motion. The temperature dependence of the mean correlation time shows an Arrhenius behaviour in the temperature range from 223 to 383 K. The activation energy at ambient pressure is 11.3 kJ mol^{-1}, which is slightly lower than the value of the barrier between the *trans* and *gauche* conformations (13.2 kJ mol^{-1}). The effect of increasing the pressure by 1 kbar corresponds roughly to lowering the temperature by 15 K.

(Keywords: deuteron n.m.r.; polyethylene; molecular dynamics)

INTRODUCTION

Solid polyethylene (PE) is the most widely studied example of a semicrystalline synthetic polymer. PE has very favourable physical and mechanical properties over a wide temperature range. The properties are intimately related to the dynamics on a molecular scale.

On the basis of various techniques, namely heat capacity, dielectric relaxation and dynamical mechanical analysis experiments, three main relaxation processes have been reported[1]. The α process is observed between 300 and 390 K and is attributed to 180° jumps accompanied by a translation of the chain stems in the crystalline phase close to the melting point. The β process occurs in branched PE in the range 240 to 280 K, however, it was also observed in linear PE. It is connected with the motion of disordered chain units, which are associated with the interfacial regions of semicrystalline PE. The γ process is observed in the range 120 to 150 K and is associated with a glass transition. There is no agreement about the precise location of the glass transition temperature[2,3] in this temperature region.

In contrast with dielectric relaxation and dynamical mechanical analysis, nuclear magnetic resonance (n.m.r.) probes molecular dynamics on a microscopic scale. Presently, n.m.r. is the only experimental method yielding detailed information about molecular order and about the type of molecular motion on the time-scale appropriate for solid polymers. This information is reflected in n.m.r. spectra[4] and relaxation rates[5]. In deuteron (^{2}H) n.m.r. in polymers the local interactions of the deuterons are dominated by the coupling between the nuclear quadrupole moment eQ and the electric field gradient (EFG) tensor at the site of the nucleus. The n.m.r. frequency is given by[5]:

$$\omega = \omega_0 \pm \delta(3\cos^2\theta - 1 + \eta\sin^2\theta\cos 2\varphi) = \omega_0 \pm \omega_Q(\theta, \varphi) \quad (1)$$

where $\omega_0 = \gamma B_0$ is the Zeeman frequency, $\delta = 3e^2qQ/8\hbar$, the quantity $e^2qQ/\hbar$ is the quadrupole coupling constant, and eq and η are the largest component and the asymmetry parameter of the EFG tensor, respectively. The polar angles θ, φ specify the orientation of the magnetic field vector B_0 in the principal axes system of the EFG tensor. In deuterated aliphatic polymers the EFG tensor is nearly axially symmetric and $\eta \simeq 0$. For PE, $e^2qQ/\hbar = 2\pi \times 164$ kHz. Since in an amorphous polymer system the orientations of the EFG tensor at the deuteron sites have an isotropic distribution, the quadrupole echo spectrum arising from the two transitions for the case of an axially symmetric tensor ($\eta = 0$) is the 'Pake doublet' typical for a static solid. Spiess and Sillescu[6] have analysed the effect of molecular motion on the timescale of the reciprocal quadrupole coupling constant on the quadrupole echo spectrum. In this paper we will make use of this analysis.

From earlier n.m.r. studies of PE we mention here the work of Hentschel *et al.*[7], who reported on a ^{2}H n.m.r. study of the chain motion in the amorphous part of PE. Spin–lattice relaxation times, quadrupole echo spectra and spin alignment echo spectra were recorded in the temperature range 123–393 K. The signals from the amorphous and crystalline fractions were separated making use of their different T_1 values. In the analysis of the spectra it was assumed that locally the conformations of the PE chain are restricted to those where carbon

* To whom correspondence should be addressed
† Present address: Unilever Research Laboratory, Physical and Analytical Sciences, Olivier van Noortlaan 120, NL-3133 AT Vlaardingen, The Netherlands

0032-3861/94/11/2307–08

atoms are placed on the sites of a diamond lattice. Then the directions of the C–^{2}H vectors lie on the four threefold symmetry axes of the lattice. Motion of the chain was introduced by diffusion of *gauche* defects along the chain. The data were analysed in terms of highly constrained conformational motions, which generate an exchange of C–^{2}H bond directions between two, three or all four tetrahedral directions on a diamond lattice. In the temperature range below 200 K only two sites are accessible; at increasing temperature the number of conformations increases, leading to an isotropic four-site exchange above 330 K.

In this paper we examine how changes in pressure and temperature affect molecular motions in linear PE by using ^{2}H n.m.r. techniques. Our aim is, first, to extend the measurements of Hentschel *et al.*[7] to high pressures and, secondly, to extract correlation times from n.m.r. line shapes.

EXPERIMENTAL

Spectrometer and high-pressure probe

Deuteron n.m.r. spectra were recorded on a home-built spectrometer at 41.43 MHz in a superconducting magnet ($B = 6.4$ T)[8].

The high-pressure probe used is described elsewhere[9]. For temperatures below 300 K the r.f. feed-through into the probe was insulated by high-molecular-weight PE; for higher temperatures we have used Vespel-SP21 (Du Pont). The sample was pressurized up to 2500 bar with nitrogen gas. The pressure was measured with an accuracy of 5 bar, using a manometer calibrated against a pressure balance, the absolute accuracy of which is better than 1:10 000. The probe was placed in a cryostat, which is also described in ref. 9. Temperatures below 293 K were obtained by cooling the cryostat with cold nitrogen gas. The temperature was controlled within 0.01 K in the whole temperature region using a PI unit.

Sample

A fully deuterated linear PE sample ($M_w = 100\,000$, $M_w/M_n = 10$; Merck, Darmstadt) was made available by Prof. Dr H. W. Spiess. The sample was machined to a diameter of 6 mm and to a length of 10 mm in order to fit into the r.f. coil inside the high-pressure n.m.r. probe.

N.m.r. spectra

Deuteron n.m.r. spectra were obtained using the quadrupole echo and spin alignment echo techniques, which have been discussed extensively in refs. 6 and 10. Spectra of the amorphous part of PE were obtained after partial recovery of the spin system from a saturating pulse sequence consisting of five $\pi/2$ pulses, separated by 2 ms. The partial recovery time was chosen to be $2T_{1a}$, where T_{1a} is the spin–lattice relaxation time of the amorphous part found already by Hentschel *et al.*[7]. T_{1a} varies between 20 and 100 ms. In the temperature range of our measurements T_1 in the crystalline region varies between 1 and 30 s (ref. 7).

We have measured two types of spectra: quadrupole echo spectra and spin alignment echo spectra. A quadrupole echo sequence $[\pi/2 - t_1 - \pi/2 - t_1 - \text{acq.}]$ was used with a variable delay t_1 of 20, 100 and 200 μs. In the spin alignment echo sequence $[\pi/2 - t_1 - \pi/4 - t_2 - \pi/4 - t_1 - \text{acq.}]$ the evolution time was $t_1 = 20\,\mu$s and the mixing time t_2 was varied between 1 and 40 ms. Both sequences are applied after the saturating sequence; the first two r.f. pulses have a phase difference $\pi/2$.

The $\pi/2$ pulse width was determined by maximizing the amplitude of the quadrupole echo. The duration of a $\pi/2$ pulse was about 4.5 μs. Transmitting more power to the probe caused electrical breakdown in the high-pressure feed-through. A $\pi/2$ pulse of 4.5 μs would lead to considerable distortion of the line shape because of insufficient excitation bandwidth[11], and therefore we used $\pi/4$ pulses instead of $\pi/2$ pulses.

The echoes were digitized in 4096 data points using quadrature detection; the spectral width was 1.25 MHz. Making use of spline functions the digitized points were shifted so that the first data point was the echo maximum[12]. Before Fourier transformation an exponential weighting corresponding to a line broadening of 2 kHz was applied. A phase cycling scheme[12] was used to suppress artifacts. Usually the number of scans was 1000.

Quadrupole echo spectra simulations

Simulations of spectra were made using a program kindly made available by Prof. Dr R. L. Vold. The full description of the program can be found elsewhere[13].

RESULTS AND ANALYSIS

Quadrupole echo spectra

Deuteron n.m.r. quadrupole echo spectra of PE as a function of temperature and pressure are shown in *Figures 1, 2* and *3*. The spectra taken at 203 K and 1500 bar are nearly equivalent to a Pake doublet. Spectra measured at ambient pressure show changes as a function of t_1, which is evidence for motion with a correlation

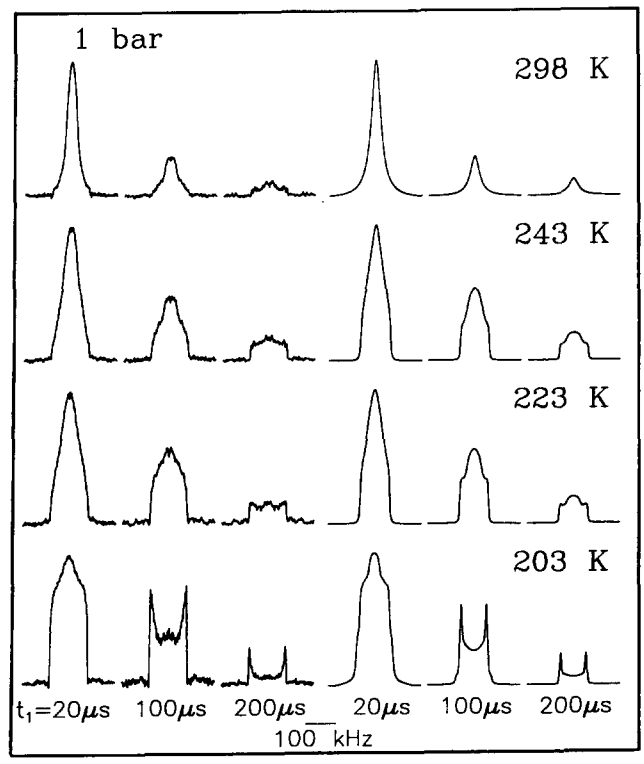

Figure 1 Experimental and simulated quadrupole echo spectra of mobile deuterons in polyethylene as a function of temperature for different pulse intervals t_1 at ambient pressure in the temperature interval 203–298 K

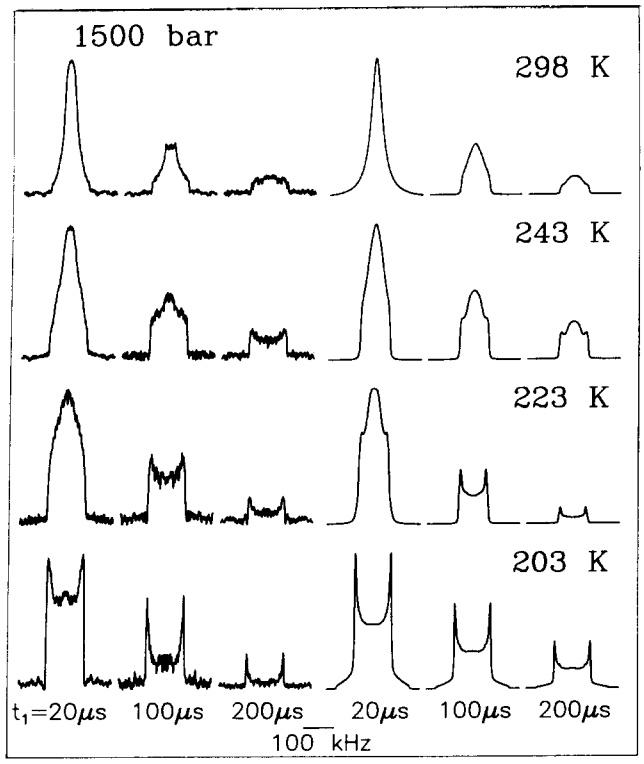

Figure 2 Experimental and simulated quadrupole echo spectra of mobile deuterons in polyethylene as a function of temperature for different pulse intervals t_1 at 1500 bar in the temperature interval 203–298 K

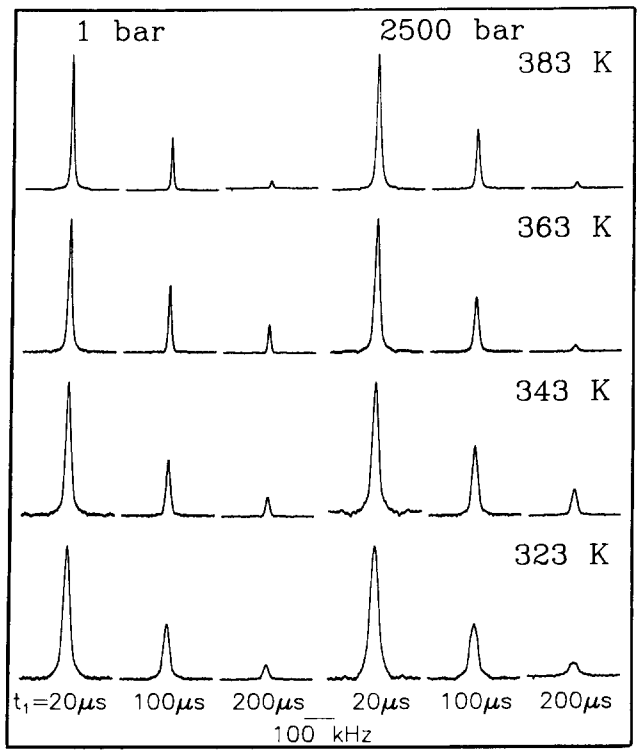

Figure 3 Experimental quadrupole echo spectra of mobile deuterons in polyethylene as a function of temperature and pressure for different pulse intervals t_1 above 323 K

time on the time-scale of the experiment. Further distortion due to molecular motion becomes apparent on increasing the temperature. At temperatures between 203 and 298 K we observe that the intensity of the quadrupole echo varies with temperature. This is caused by a change of the reduction factor of the echo amplitude, which is also an indicator of molecular motion. At 323 K the spectra are averaged to a single structureless line. As the temperature is increased above 323 K, the lineshape continues to sharpen. The effect of pressure is similar to lowering the temperature. It also slows down the motion. Above 323 K application of pressure only results in broadening of the line.

Model for quadrupole echo spectra simulations

In order to obtain detailed information about the type and the time-scale of the motion, we have compared experimental and simulated spectra. Our simulations are based on the 'rotational isomeric state model' (RIS model) of the PE chain developed by Flory[14]. There, the conformational energies of n-pentane have been calculated as a function of their C–C bond rotation angles using expressions for the repulsive and attractive energies between non-bonded atom pairs and an intrinsic three-fold torsion potential $V(\varphi)=V_0(1-3\cos\varphi)$. With these assumptions Flory and coworkers[15] have calculated the energy map for the internal rotations of n-pentane. As the result of these calculations it was shown that the rotations of the chain are not limited to the three well known rotational isomeric states, *trans* (t) at $\varphi=0°$ and *gauche*$^{\pm}$ ($g^{\pm}$) at $\varphi=112.5°\pm3°$, but that five energy minima exist. These minima are incorporated in a five-state scheme comprising rotational states t, g_*^+, g^+, g^- and g_*^- at angles $\varphi=0$, 80, 115, -115 and $-80°$, respectively. They correspond to the following energy minima with respect to the t state: $g^{\pm}\approx2.2\,\mathrm{kJ\,mol^{-1}}$, $g_*^{\pm}\approx13.4\,\mathrm{kJ\,mol^{-1}}$. Owing to the fact that the interdependence of bond rotations is limited to first-neighbour bonds[14], the conformational energies found in n-pentane also occur in n-alkane molecules of any length, including polyethylene. We note here that the potential minima have been calculated for a free molecule. As stated by Flory, this, on average, also holds in the liquid. It is reasonable to assume that in the amorphous solid phase the values of the minima will be affected by the intermolecular interactions and will show a distribution about their average values. In our analysis we assume that these average values have the same values as in the free molecule and that we can incorporate the effect of the distribution of minimum values by introducing a distribution of times between conformational transitions.

The uncertainties in the values of the carbon bond angles at which the potential minima are found in these calculations are $\pm3°$. We have included this in our simulations by assuming an additional Gaussian distribution in the potential minima with a standard deviation of $\Delta\varphi=1.5°$. The changes caused by slightly different jump angles are small but not negligible and therefore are included in our model calculations. In the simulations of the spectra we have assumed that the C–^{2}H bond makes discrete reorientations over three or five directions on a cone about the flip axis. The opening angle of the cone is the angle between the z-axis of the EFG tensor and the flip axis, which is 68°. We have used this value since a carbon–carbon bond angle is 112°, in accordance with observations by X-ray spectroscopy[16].

As a consequence of the RIS model, the *a priori* populations of each of the potential minima are unequal. Moreover, they are a function of temperature. At temperatures below 150 K the populations of the g_*^+, g_*^- states are nearly zero and thus can be neglected. This

Table 1 *A priori* probabilities used in the simulations

	t	g_*^+	g^+	g^-	g_*^-
Three states	0.80	–	0.10	0.10	–
Five states	0.58	0.03	0.18	0.18	0.03

reduces the model to the three well-known rotational isomeric states. On increasing the temperature the *a priori* probabilities of the g_*^+, g_*^- states become non-negligible and we have included them in our simulations. We have tried to keep our calculations as simple as possible, and therefore we have calculated spectra for two sets of *a priori* probabilities, one for the three-state model and one for the five-state model, calculated at 150 and 300 K, respectively. They are summarized in *Table 1*.

Transitions between the conformations are characterized by a jump matrix, the non-diagonal elements of which describe the rate of jumps from state j to i and the diagonal elements of which are the negative sum of all rates that deplete state i. In the simulations care is taken that the elements of the jump matrix satisfy the microscopic reversibility equation[17].

The molecular motion is characterized by the mean time intervals of the transitions between different conformational states. In the simulations of the spectra we derive the transition rates in the three-state and in the five-state model from an average value of the time between jumps $\tau = P_i\tau_i$, where P_i is the *a priori* probability at state i, τ_i is the time interval of the transitions from site i and $i=1,\ldots,n$ where n is the number of states. In our simulations we have assumed an asymmetric distribution of τ on a logarithmic scale, namely a log-Gaussian truncated for large τ values from its maximum value. The expression for a log-Gaussian is given by:

$$\rho(\ln\tau) = \frac{1}{\sigma(2\pi)^{1/2}}\exp\left(-\frac{(\ln\tau - \ln\tau_0)^2}{2\sigma^2}\right) \qquad (2)$$

where $\ln\tau_0$ is the mean logarithm of the time interval between conformational transitions and 2σ is the width of the distribution on a logarithmic scale. In the following we use the width $\Delta = 2\sigma\log e$ in decades. In practice the continuous distribution was replaced by a discrete one by calculating spectra for 11 values of τ spanning the whole width of the distribution[18]. A spectrum for a given mean correlation time and distribution width was obtained by summing 11 spectra weighted by the truncated log-Gaussian distribution (2). We note here that this distribution resembles a Kohlrausch–Williams–Watts (KWW)[19] distribution of correlation times, especially for values of the parameter $\beta > 0.6$. The KWW distribution is given by the inverse Laplace transform of $q(t) = q(0)\exp[-(t/\tau)^\beta]$ with $\beta \in (0; 1)$. The use of a log-Gaussian has the advantage that it can be easily calculated, in contrast with calculations of the KWW distribution, which are unstable for values of $\beta > 0.5$ (ref. 20). In our fitting procedure we have assumed a variation of the width of the distribution, starting from $\Delta = 2.6$ at $T = 203$ K to $\Delta = 0.4$ at $T = 383$ K. Clearly we want the simulated spectra to fit the experimental ones for all values of t_1 in the quadrupole echo experiment, using τ_0 and σ as the fitting parameters. The quality of the fit can be seen from the comparison of the simulated and experimental spectra in *Figures 1* and *2*.

Analysis of the quadrupole echo spectra

At 203 K, the simulated spectra have been calculated using the three-state model; the five-state model results in a less satisfactory fit. At ambient pressure we see a clear change of shape on the time-scale of the quadrupole echo experiment, while an increase of pressure of 1500 bar results in a 'Pake'-like line shape for all values of t_1 apart from a loss of intensity in the middle of the spectrum. This loss of intensity cannot be reproduced in the spectra calculated according to the model introduced above. We return to this point in the discussion.

At 223 K and 1500 bar again the fit was much better for the model including motion between three states instead of motion over five states. As can be seen from *Figures 1* and *2* the changes of the spectra as a function of t_1 are similar to those at $T = 203$ K, $p = 1$ bar. The spectra at $T = 223$ K and $p = 1$ bar and $T = 243$ K, $p = 1500$ bar are nearly the same, so we describe these line shapes with the same parameters. However, in these two cases the five-state model gives the best result. Also the simulation to fit the spectra measured at ambient pressure at $T = 243$ K is made with the five-state model.

At a temperature of 298 K there is a cross-over to a structureless line. This can be observed, for instance, by inspection of the spectra measured at 1500 bar. There, the spectrum at $t_1 = 20\,\mu$s is a nearly Lorentzian line, while the spectrum at $t_1 = 100\,\mu$s has a shape similar to the one at 243 K. For this temperature value we have made fits to the experimental spectra with spectra calculated for the five-state motion and to a Lorentzian line shape (as is explained in the next paragraph), using the same characteristic time τ and width Δ. At ambient pressure a better fit is obtained with a Lorentzian, at $p = 1500$ bar only at $t_1 = 20\,\mu$s does a Lorentzian fit better, while at the two other t_1 values the spectra calculated with the five-state model give a better fit.

As has been mentioned above, the characteristic features of the quadrupole echo line shape are lost at a temperature of 298 K and above. The line becomes structureless and almost completely Lorentzian. This cannot be due only to the jump rate becoming fast. Presumably, the loss of structure is caused by a loss of restrictions on the jump motion at higher temperature. The distribution of allowed orientations, initially restricted to three or five orientations on a cone, becomes less discrete. At higher temperatures anisotropic reorientation becomes a better model for the motion. The angular dependence of the quadrupole coupling is given by the second-order spherical harmonic $3\cos^2\theta - 1$. Averaging of the spherical harmonic to zero can occur not only for isotropic motion but also for restricted motion (e.g. motion consisting of jumps between four positions on a cone with the tetrahedral angle). Therefore, it is reasonable to assume that the anisotropic motion of the PE chain above 298 K is sufficient to average the line shape to a Lorentzian. For simplicity, we have assumed that the motion of the C–D bond is isotropic diffusion, characterized by a log-Gaussian distribution of correlation times τ_c. We therefore fit the spectra with a superposition of Lorentzians $(1 + \Delta\omega^2 T_2^2)^{-1}$. The relation between a correlation time τ_c and the transverse spin relaxation rate is given by[6]:

$$\frac{1}{T_2} = \frac{3}{80}\left(\frac{e^2qQ}{\hbar}\right)^2\left(3\tau_c + \frac{5\tau_c}{1+\omega^2\tau_c^2} + \frac{2\tau_c}{1+4\omega^2\tau_c^2}\right) \qquad (3)$$

The results should be taken with some reservation, owing

to the simplifications made in obtaining the correlation times from the lineshapes. The character of the motion changes as a function of temperature, becoming more isotropic at increasing temperature. In addition, the theory of relaxation leading to (3) is based on the differential equation for the density matrix[6], which is valid only for sufficiently small values of τ_c such that $|H_Q\tau_c|^2 \ll 1$, where $\hbar H_Q$ is the quadrupole coupling Hamiltonian. This means that τ_c should be much shorter than 1 μs. The correlation times obtained are on the limit of the validity of the density matrix equation. In fact, the condition $|H_Q\tau_c|^2 \ll 1$ only starts to be valid in the region of our measurements.

We stress that the correlation time τ_c in equation (3) is different from the mean time τ between jumps introduced above; τ_c is the correlation time of a second-order spherical harmonic, subject to reorientational diffusion, $\tau_c = (6D_r)^{-1}$. Nevertheless, these parameters characterize the time-scale of the same process, which gradually loses its discrete nature. For simplicity, we will disregard the distinction in the remainder of this paper and we will use τ_c to designate the characteristic time.

The numerical results obtained from the comparison of the experimental and simulated spectra are collected in *Table 2*.

Activated processes

Assuming that each type of conformational transition of the chain is an activated process, the mean time between jumps is given by an expression of the Arrhenius form:

$$\tau_c = \tau' \exp(\Delta G/RT) \tag{4}$$

where ΔG is the free enthalpy of activation, $\Delta G = \Delta E + p\Delta V - T\Delta S$, where ΔE, ΔV and ΔS are the energy, volume and entropy of activation, respectively. In the following we disregard the fact that ΔG is different for different types of conformational transitions. In analogy with the analysis of vacancy diffusion[21], we identify ΔE with the energy barrier; the activation volume ΔV consists of the expansion of the system at the saddle-point configuration. For the three-state model, we assume that ΔE is the energy barrier for a t to $g^{\pm}$ conformational transition.

As has been shown above, the motion is characterized by a distribution of characteristic times. These distributions reflect local variations of the activation parameters and depend on temperature and pressure. Therefore, a detailed analysis of the data in terms of the activation parameters is not possible. Instead, we have derived

Table 2 Correlation times τ_0 (μs) and distribution widths Δ (decades) used in the comparison of simulated and experimental quadrupole echo spectra

	1 bar		1500 bar	
T(K)	τ_0	Δ	τ_0	Δ
203	33.00	2.4	10 000.00	2.6
223	2.00	2.0	12.50	2.2
243	1.25	1.5	2.00	2.0
298	0.80	0.4	1.40	1.0
323	0.50	0.4	0.72	0.5
343	0.35	0.3	0.53	0.3
363	0.25	0.3	0.35	0.3
383	0.16	0.2	0.26	0.3

Table 3 Activation enthalpy ΔH for molecular motion in amorphous PE

p(bar)	ΔH(kJ mol^{-1})
1	11.4±1.4
1500	15.6±1.6

Table 4 Activation volume ΔV for molecular motion in amorphous PE

T(K)	ΔV(cm^3 mol^{-1})
223	17.8±1.8
243	11.8±1.2
298	9.5±1.0
323	6.7±0.7
343	8.0±0.8
363	6.9±0.7
383	10.3±1.1

'average' activation parameters from equation (4), using the values of τ_c from *Table 2*. If one assumes that τ', ΔE, ΔV and ΔS are independent of temperature, one can calculate the activation enthalpy $\Delta H = \Delta E + p\Delta V$ from:

$$\Delta H = R\left(\frac{\partial \ln \tau_c}{\partial T^{-1}}\right)_p \tag{5}$$

From the data in the temperature interval 223–383 K we obtain the results presented in *Table 3*. The activation volume in this temperature range is obtained from:

$$\Delta V = RT\left(\frac{\partial \ln \tau_c}{\partial p}\right)_T \tag{6}$$

Values of ΔV calculated from the τ_c values are collected in *Table 4*.

At ambient pressure the ΔH value found for the motion is 11.4±1.4 kJ mol^{-1}. The $p\Delta V$ contribution to ΔH at 1 bar is only about 0.1 kJ mol^{-1}, so ΔE is 11.3 kJ mol^{-1}, a value that is somewhat lower than the value of the barrier between t and $g^{\pm}$ conformations observed in free alkanes, which is 13.2 kJ mol^{-1} (refs. 14, 15).

Spin alignment echo spectra

Figures 4 and *5* show the spin alignment echo spectra as a function of pressure and temperature. The lineshapes obtained at 203 K and 1500 bar are Pake doublets corresponding to complete freezing of the motion. The spectra recorded at 203 K at ambient pressure show changes as a function of t_m. This process continues on increasing the temperature. Above 298 K the spin alignment lineshapes are independent of t_m; narrowing of the line is caused by further averaging of the EFG tensor resulting in a Lorentzian shape. The decay of the signal is governed by T_{1Q}, which is nearly equal to T_1. Spin alignment remains detectable up to 40 ms just before the melting point at 383 K. This means that a non-vanishing average EFG tensor persists on the timescale of the experiment. The effect of increasing the pressure is roughly similar to the effect of lowering the temperature.

The changes of the line shape as a function of t_m are an indication of motion on the time-scale of the experiment (milliseconds). These times, however, lie outside the distribution of correlation times found by the quadrupole echo experiments discussed above. Therefore, the changes of the line shape have another origin. They have been attributed before to the motion of long-lived topological constraints[7]. Presumably, the motion of the constraints

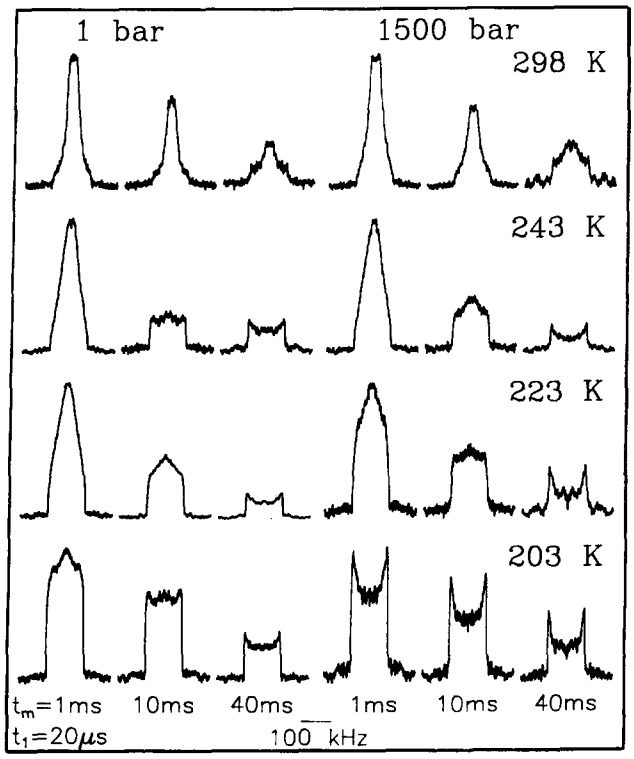

Figure 4 Experimental spin alignment echo spectra of mobile deuterons in polyethylene below 300 K as a function of pressure and temperature for different mixing times t_m

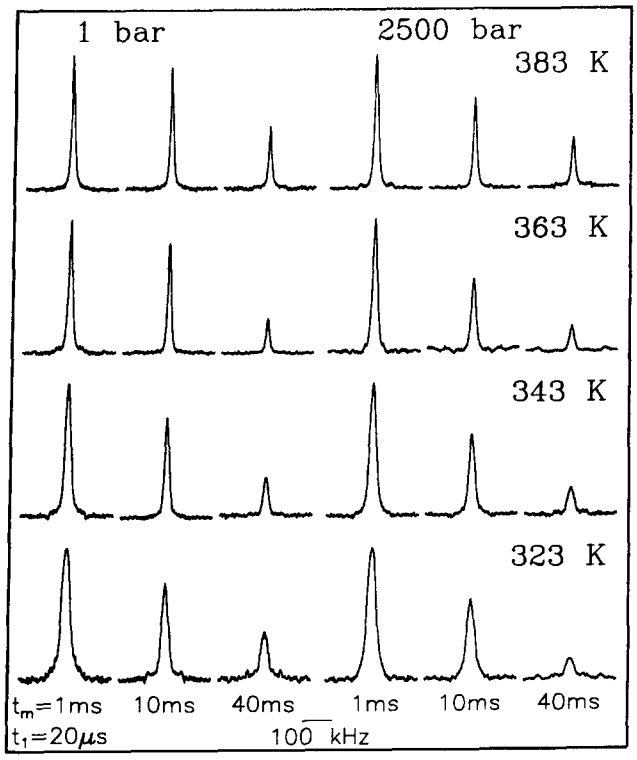

Figure 5 Experimental spin alignment echo spectra of mobile deuterons in polyethylene above 300 K as a function of pressure and temperature for different mixing times t_m

leads to slow reorientational motion of the chain, which is superimposed on the motion discussed above. Finally, it also leads to complete averaging of the line. A somewhat similar situation was found in polycarbonate-d_4, where a dominant role is played by the fast flips of the phenylene rings on the time-scale of the quadrupole echo experiment, but slow molecular reorientations can be detected in a 2D exchange experiment[22].

DISCUSSION

Nature of the motion

Our analysis of ^2H n.m.r. data shows that chain motion in the amorphous part of PE is highly restricted. In particular, at the lowest temperatures of our measurements the C–^2H bonds are almost completely arrested in the structure.

At $T=203$ K the only observable effect of motion on the quadrupole echo spectra is a loss of intensity in the middle, which cannot be due to discrete conformational changes of the PE chain. Usually, such changes are attributed to small-angle rotational diffusive motion[6]. A similar effect was found in polystyrene[23,24] and polypropylene[25,26]. There, it was observed that just above the glass transition temperature the chain starts to perform small-angle reorientational diffusive motion. This is caused by the fact that near to and above the glass transition the motion is not a strictly local process described by motions about well defined angles but is due to the relaxation processes involving larger chain units, leading to translational and angular displacements of different amplitudes[27]. In PE the glass transition temperature has been reported to be at about 150 K[28]. Therefore, it is not surprising that we observe changes in the spectra that can be attributed to small-angle reorientational diffusive motion. We expect that at 203 K and 1500 bar we are close to the glass transition, although according to the spectra the motion has not yet stopped.

On increasing the temperature, conformational changes occur, and in addition there are changes in the equilibrium populations of the rotational isomeric states. This allows us to describe the motion at 203 K by the three-state model; in the temperature range 223–298 K we use the five-state model.

Above 298 K the conformational transitions in the amorphous part of PE become less discrete, such that the motion can be approximated by quasi-isotropic diffusion. The analysis of the line shapes above 298 K is based upon the assumption that the observed residual linewidth is homogeneous in nature.

The analysis, which involves the merging of two regimes of motion as described above, leads to the interesting result that the motion can be regarded as a single Arrhenius process over a large temperature interval, namely from 223 to 383 K (see *Figure 6*).

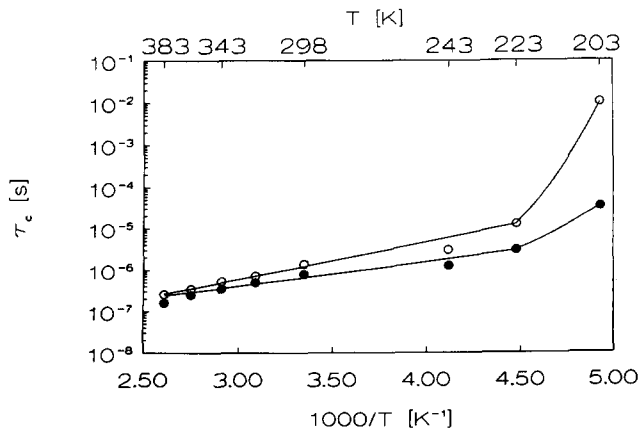

Figure 6 Logarithmic mean characteristic time for the transitions between different conformational states: (●) 1 bar, (○) 1500 bar

As can be seen from the spectra in *Figures 1, 2* and *3* the changes in the accessible conformations result in drastic changes of the line shape. The constraints in the motion are caused by the packing of the chains and the interaction between neighbouring chains. Similarly in the simulations of PE chains it was shown recently[29] that the occurrence of conformational disorder is a gradual process, which changes continuously with increasing temperature and decreasing density.

Comparison with other motional models

As has been mentioned already in the 'Introduction', another model for the description of the *trans–gauche* isomerization of PE is possible by allowing transitions between conformations of the chain that are compatible with those of a diamond lattice. Two kinds of motion are introduced, kink (two-site exchange) and crankshaft (three-site exchange) motion[30]. Kink motion is a chain motion where three bonds take part and one *gauche* defect is required. The C–^{2}H bond reorients over 180° on a cone about the flip axis. The principal z-axis of the EFG tensor remains oriented at 54.7° relative to the flip axis. Crankshaft motion is a five-bond motion. Within these five bonds two *gauche* defects are needed. On a diamond lattice the principal z-axis of the tensor makes an angle of 70.3° with the flip axis for crankshaft motion. The C–^{2}H bonds reorient over 120° on a cone about the flip axis. This type of reorientation is the same as for the three-state motion in the rotational isomeric state model. We have performed such a calculation following these ideas.

In order to obtain a fit of the spectra, we adjust the fractions of the contributions of flexible chain units showing kink motion, crankshaft motion and of the chain units remaining rigid. Furthermore, log-Gaussian distributions of mean jump times in both the kink and crankshaft fractions are assumed. The results for the temperature interval 203–298 K are presented in *Figure 7*, which shows the fractions of the various flexible units present at a number of temperature and pressure values[8]. The number of bonds taking part in the motion increases on increasing the temperature and decreases on increasing the pressure. As before, discrete kink and crankshaft motion cannot account for the structureless quadrupole echo spectra obtained in the temperature range 323–383 K. In this temperature interval we have the results obtained via equation (4), as discussed above.

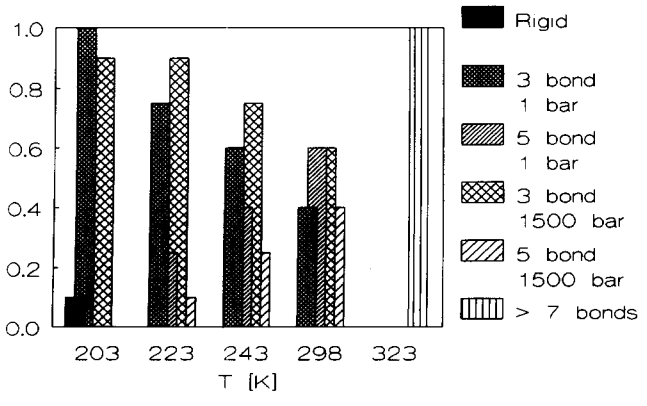

Figure 7 Fractions of flexible units in the amorphous part of polyethylene as obtained from the comparison of simulated and experimental quadrupole echo spectra

We note that in the model allowing motion on a diamond lattice the quality of the fit of the simulated spectra to the experimental spectra is much poorer than in the rotational isomeric state model.

We would also like to mention that the quadrupole echo line shapes obtained in our experiments are similar to those obtained by Hirschinger *et al.*[31] in a ^{2}H n.m.r. study of selectively deuterated crystalline nylon-6,6. There, line shapes have been calculated for a Gaussian librational model of segmental motion. It is assumed that the C-^{2}H group within the chain can fluctuate around the local C–C bond by a Gaussian distribution of librational angles, $P(\theta)$, with standard deviation $\Delta\theta$. In fitting the spectra it was assumed that the standard deviation $\Delta\theta$ itself is inhomogeneous indicating that the motion is spatially inhomogeneous.

From our model calculations and the model presented above, it may be concluded that the reproduction of the experimental spectra by simulated spectra, within the accuracy of both, is not unique. This is due to the fact that the orientation dependence of the n.m.r. frequency given in equation (1) goes (for $\eta=0$) as the second-order Legendre polynomial and one can figure out many motional models that will average (1) in the same way.

Pressure dependence

The results summarized in *Table 2* show a gradual increase of the mean correlation time and distribution width at increasing pressure, showing the motional restrictions introduced by pressure. In the temperature range of our measurements we have found that the application of 1 kbar of hydrostatic pressure produces an increase of the correlation times roughly corresponding to a decrease of temperature of about 15 K. At all temperatures the effect of pressure on the molecular motion is reversible.

The ΔH value found for the motion at 1 bar is 11.4 kJ mol^{-1} as shown in *Table 3*. Our analysis yields that the ΔH value at 1500 bar is 15.6 kJ mol^{-1}. Taking into account a value of the activation volume of about 10 cm^3 mol^{-1}, we calculate the contribution of the $p\Delta V$ term to ΔH to be about 1.5 kJ mol^{-1}. Presumably, the remaining difference is caused by the increase of the energy barrier ΔE on increasing the density. The compressibility in this temperature range is only about 0.019 kbar^{-1}.

The activation volumes ΔV collected in *Table 4* should be compared with the value 14.1 cm^3 mol^{-1} of the molecular repeat unit (–CH_2–) as determined from X-ray diffraction data[32] measured at ambient pressure and temperature. It can be seen that the ΔV values are temperature-dependent, however, the ΔV value remains close to the molecular repeat-unit volume. As has been mentioned before, ΔV consists of the expansion of the system at the saddle-point configuration and of the volume increase involved in the creation of the chain defects, necessary for that type of motion. At 223 K, ΔV has the highest value since there the packing of the chains is dense and they are immobile. This requires a large extra volume for reorientation. On increasing the temperature the packing of the chains gets less dense and molecular motion gets faster. This results in a decrease of ΔV up to 323 K. At this temperature we observe a change in the type of chain motion. Motion becomes quasi-isotropic, which presumably requires cooperative motion of flexible chain units. We suggest that the observed

increase of ΔV with temperature above 323 K is an indicator of the strong dependence of the length of the flexible chain units on temperature.

REFERENCES

1 Axelson, D. E. in 'High Resolution NMR Spectroscopy of Synthetic Polymers in Bulk' (Ed. R. A. Komoroski), VCH Publishers, Deerfield Beach, 1986, Ch. 5.1
2 Gaur, U. and Wunderlich, B. *Macromolecules* 1980, **13**, 445
3 Beatty, C. L. and Karasz, F. E. *J. Macromol. Sci., Rev. Macromol. Chem.* 1979, **17**, 37
4 Spiess, H. W. *Chem. Rev.* 1991, **91**, 1321
5 Abragam, A. 'The Principles of Nuclear Magnetism', Clarendon Press, London, 1961
6 Spiess, H. W. and Sillescu, H. *J. Magn. Reson.* 1980, **42**, 381
7 Hentschel, D., Sillescu, H. and Spiess, H. W. *Polymer* 1984, **25**, 1078
8 Kulik, A. S. PhD Thesis, University of Amsterdam, 1992
9 Prins, K. O. in 'NMR Basic Principles and Progress' (Eds. P. Diehl, E. Fluck, H. Günther, R. Kosfeld and J. Seelig), Springer, Berlin, 1991, Vol. 24, p. 29
10 Spiess, H. W. *J. Chem. Phys.* 1980, **72**, 6755
11 Bloom, M., Davis, J. H. and Valic, M. I. *Can. J. Phys.* 1980, **58**, 1510
12 Ronemus, A. D., Vold, R. L. and Vold, R. R. *J. Magn. Reson.* 1986, **70**, 416
13 Greenfield, M. S., Ronemus, A. D., Vold, R. L., Vold, R. R., Ellis, P. D. and Raidy, T. E. *J. Magn. Reson.* 1987, **72**, 89
14 Flory, P. J. 'Statistical Mechanics of Chain Molecules', Carl Hanser, Munich, 1988
15 Abe, A., Jernigan, R. L. and Flory, P. J. *J. Am. Chem. Soc.* 1966, **88**, 631
16 Schearer, H. M. M. and Vand, V. *Acta Crystallogr.* 1956, **9**, 379
17 Wittebort, R. J., Olejniczak, E. T. and Griffin, R. G. *J. Chem. Phys.* 1987, **86**, 5411
18 Schmidt, C., Kuhn, K. J. and Spiess, H. W. *Prog. Colloid Polym. Sci.* 1985, **71**, 71
19 Williams, G. and Watts, D. C. *Trans. Faraday Soc.* 1970, **66**, 80
20 Linsey, C. P. and Patterson, G. D. *J. Chem. Phys.* 1980, **73**, 3348
21 Flynn, C. P. 'Point Defects and Diffusion', Clarendon Press, Oxford, 1972
22 Hansen, M. T., Blümich, B., Boeffel, C., Spiess, H. W., Morbitzer, L. and Zembrod, A. *Macromolecules* 1992, **25**, 5542
23 Kulik, A. S. and Prins, K. O. *Polymer* 1993, **34**, 4629
24 Pschorn, U., Rössler, E., Sillescu, H., Kaufmann, S., Schaefer, D. and Spiess, H. W. *Macromolecules* 1991, **24**, 398
25 Schaefer, D., Spiess, H. W., Suter, U. W. and Fleming, W. W. *Macromolecules* 1990, **23**, 3431
26 Zemke, K., Chmelka, B. F., Schmidt-Rohr, K. and Spiess, H. W. *Macromolecules* 1991, **24**, 6874
27 Helfand, E., Wasserman, Z. R., Weber, T. A., Skolnick, J. and Runnels, J. H. *J. Chem. Phys.* 1981, **75**, 4441
28 Stehling, F. C. and Mandelkern, L. *Macromolecules* 1970, **3**, 242
29 Sumpter, B. G., Noid, D. W. and Wunderlich, B. *J. Chem. Phys.* 1990, **93**, 6875
30 Rosenke, K., Sillescu, H. and Spiess, H. W. *Polymer* 1980, **21**, 757
31 Hirschinger, J., Miura, H., Gardner, K. H. and English, A. D. *Macromolecules* 1990, **23**, 2153
32 Young, R. J. 'Introduction to Polymers', Chapman and Hall, London, 1981